

# Molecular Meccano, 52<sup>l±l</sup>

## Template-Directed Synthesis of a Rotacatenane

David B. Amabilino,<sup>[a]</sup> Peter R. Ashton,<sup>[a]</sup> José A. Bravo,<sup>[b]</sup> Francisco M. Raymo,<sup>[b]</sup>  
J. Fraser Stoddart,<sup>\*[b]</sup> Andrew J. P. White,<sup>[c]</sup> and David J. Williams<sup>\*[c]</sup>

**Keywords:** Catenanes / Mechanically interlocked molecules / Molecular recognition / Rotaxanes / Template-directed synthesis

A [2]catenane, able to bind  $\pi$ -electron-rich guests inside the cavity of one of its two macrocyclic components has been designed and synthesized using supramolecular assistance. This recognition motif has been exploited to template the formation of a so-called rotacatenane – i.e., a molecule composed of a dumbbell-shaped component threaded through the cavity of one of the two mechanically interlocked

macrocyclic components of a [2]catenane. The structure of this [2]catenane, as well as that of a model [2]catenane, have been characterized unequivocally by single-crystal X-ray analyses. Furthermore, some of the co-conformational changes associated with these mechanically interlocked molecules in solution have been probed by variable-temperature <sup>1</sup>H-NMR spectroscopy.

### Introduction

The [2]catenane **1** · 4 PF<sub>6</sub> (Figure 1) was obtained<sup>[1]</sup> as a side product in the two-step template-directed synthesis of oligocatenanes incorporating from four up to seven mechanically interlocked<sup>[2]</sup> macrocycles. This [2]catenane is composed of a 1,5-dioxynaphthalene-based macrocyclic polyether and of a bipyridinium-based tetracationic cyclophane.<sup>[3]</sup> The two macrocyclic components are held together by a mechanical bond reinforced by (i) [C–H···O] hydrogen bonds between the  $\alpha$ -bipyridinium hydrogen atoms and the polyether oxygen atoms, (ii) [ $\pi$ ··· $\pi$ ] stacking between the  $\pi$ -electron-rich and -deficient units, and (iii) [C–H··· $\pi$ ] interactions between the hydrogen atoms of the 1,5-dioxynaphthalene unit located inside the cavity of the tetracationic cyclophane and the *p*-phenylene rings. The cavities of the mechanically interlocked macrocycles of **1** · 4 PF<sub>6</sub> are large enough to accommodate (Figure 1)  $\pi$ -electron-rich and -deficient aromatic substrates, as revealed<sup>[1]</sup> by preliminary complexation studies. Inspired by these observations, we identified (Figure 1) a mechanically interlocked receptor for  $\pi$ -electron-rich aromatic substrates in the shape of the [2]catenane **2** · 4 PF<sub>6</sub>. Here, we report (i) the template-directed synthesis of **2** · 4 PF<sub>6</sub>, (ii) its ability to

bind a 1,5-dioxynaphthalene-based polyether guest and the post-assembly covalent modification of the corresponding supramolecular complex into a rotacatenane **7** · 4 PF<sub>6</sub>, (iii) the X-ray crystallographic analysis of the [2]catenanes **1** · 4 PF<sub>6</sub> and **2** · 4 PF<sub>6</sub>, and (iv) the variable-temperature <sup>1</sup>H-NMR-spectroscopic investigation of the dynamic processes associated with both the [2]catenane **2** · 4 PF<sub>6</sub> and with the rotacatenane **7** · 4 PF<sub>6</sub> in solution.

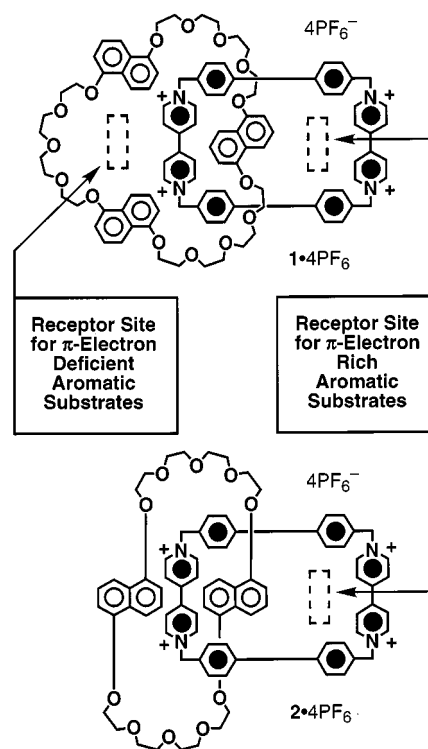


Figure 1. The [2]catenanes **1** · 4 PF<sub>6</sub> and **2** · 4 PF<sub>6</sub>

[\*] Part 51: P. R. Ashton, A. M. Heiss, D. Pasini, F. M. Raymo, A. N. Shipway, J. F. Stoddart, N. Spencer, *Eur. J. Org. Chem.* **1999**, 995–1004.

[a] School of Chemistry, University of Birmingham, Edgbaston, Birmingham B15 2TT, UK

[b] Department of Chemistry and Biochemistry, University of California, Los Angeles, 405 Hilgard Avenue, Los Angeles, CA 90095-1569, USA  
Fax: (internat.) + 1-310/206-1843  
E-mail: stoddart@chem.ucla.edu

[c] Department of Chemistry, Imperial College, South Kensington, London SW7 2AY, UK  
Fax: (internat.) + 44-171/594-5835

## Results and Discussion

## Synthesis

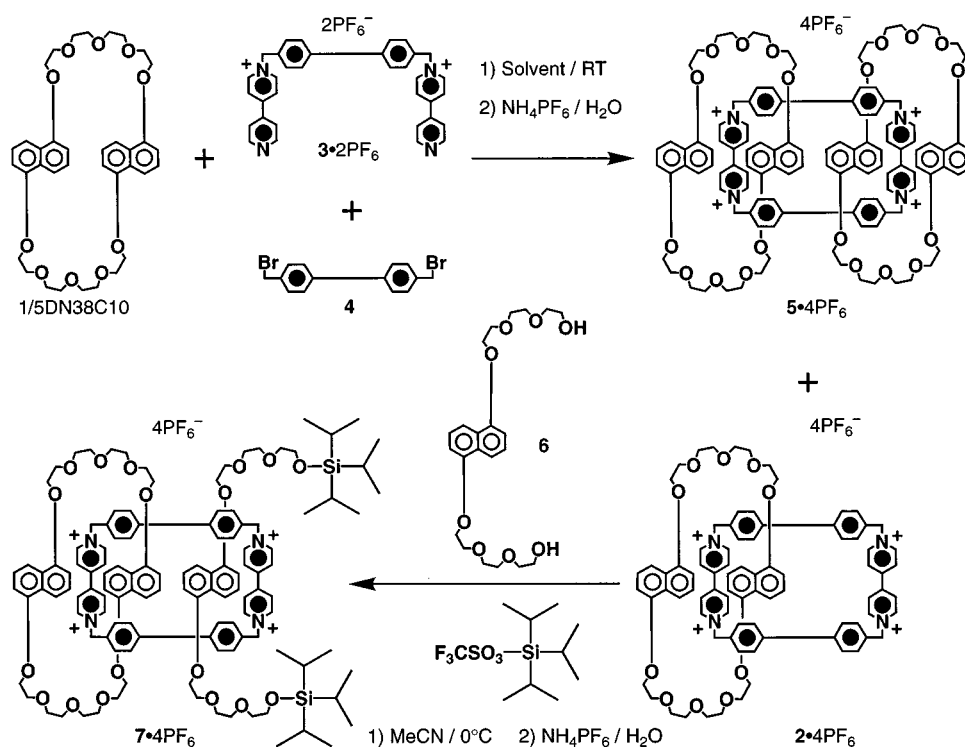
Reaction of  $3 \cdot 2 \text{PF}_6$  with **4** in the presence of 1,5-dioxynaphtho-38-crown-10 (1/5DN38C10) gave (Scheme 1) the [2]catenane  $2 \cdot 4 \text{PF}_6$  in addition to the [3]catenane<sup>[4]</sup>  $5 \cdot 4 \text{PF}_6$ , after counterion exchange. On mixing the [2]catenane  $2 \cdot 4 \text{PF}_6$  in MeCN with the  $\pi$ -electron rich guest **6**, complexation occurs. Addition of triisopropylsilyl triflate to this solution at  $0^\circ\text{C}$  afforded the rotacatenane  $7 \cdot 4 \text{PF}_6$  after counterion exchange in a yield of 40%.

## X-ray Crystallography

Unfortunately, crystals of  $1 \cdot 4 \text{PF}_6$  were of limited quality and the resulting data somewhat poor but, nonetheless, sufficient to enable an unambiguous assignment of the molecular structure (Figure 2) and supramolecular superstructure. The tetracationic cyclophane has an "open" geometry with separations of ca. 11.1 and 10.8 Å between its bipyridinium and biphenylene units, respectively. One of the bipyridinium units is encircled by the interlocking macrocyclic polyether and sandwiched between two of the three 1,5-dioxynaphthalene ring systems: the interplanar separations between the bipyridinium unit and the "inside" and "alongside" 1,5-dioxynaphthalene ring systems are 3.48 and 3.47 Å, respectively. Because of the limited accuracy of the structure determination, we have not analyzed the geometries of the intracatenane  $[\text{C}-\text{H}\cdots\text{O}]$  and  $[\text{C}-\text{H}\cdots\pi]$  interactions, though some are clearly present. The [2]catenane molecules pack to form two-dimensional  $\pi$ -stacked arrays. In one di-

rection, the "alongside" 1,5-dioxynaphthalene ring system of one molecule is positioned adjacent to the "alongside" bipyridinium unit of the next (the  $[\pi\cdots\pi]$  separation is 3.40 Å) to form polar stacks. – in the other direction, pairs of  $\text{C}_2$ -related biphenylene units are positioned parallel with phenylene rings overlapping (the  $[\pi\cdots\pi]$  separation between one pair of biphenylene units is 3.46 Å and between the other pair is 3.47 Å). Intersheet edge-to-face interactions between one of the biphenylene units in one sheet and the 1,5-dioxynaphthalene ring system, not involved in  $\pi$ -stacking in the next, are also observed (the [ring centroid $\cdots$ ring centroid] separation is ca. 4.74 Å).

The X-ray analysis of the [2]catenane  $2 \cdot 4 \text{PF}_6$  shows (Figure 3) the tetracationic cyclophane to adopt an "open" geometry with separations of 10.8 and 11.0 Å between its bipyridinium and biphenylene units, respectively. The interlocked macrocyclic polyether encircles one of the bipyridinium units with interplanar separations between this unit and the "inside" and "alongside" 1,5-dioxynaphthalene ring systems of 3.38 and 3.41 Å, respectively. Additional stabilization occurs by  $[\text{C}-\text{H}\cdots\pi]$  interactions between the *peri*-hydrogen atoms of the "inside" 1,5-dioxynaphthalene ring system and their proximal *p*-phenylene rings in the tetracationic cyclophane (the  $[\text{H}\cdots\pi]$  distances are 2.77 and 2.78 Å with associated  $[\text{C}-\text{H}\cdots\pi]$  angles of  $145^\circ$  and  $159^\circ$ , respectively). These interactions are supplemented by  $[\text{C}-\text{H}\cdots\text{O}]$  hydrogen bonds involving  $\alpha$ -bipyridinium hydrogen atoms, and also one of the corner methylene groups, and oxygen atoms in the polyether chains (the  $[\text{H}\cdots\text{O}]$  distances are in the range 2.21–2.46 Å with  $[\text{C}-\text{H}\cdots\text{O}]$  angles between  $146^\circ$  and  $149^\circ$ ). The [2]catenane molecules pack to



Scheme 1. Template-directed synthesis of the rotacatenane  $7 \cdot 4 \text{PF}_6$

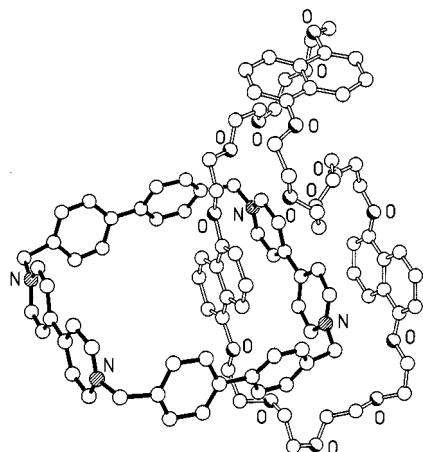


Figure 2. Ball-and-stick representation of the geometry adopted by  $1^{4+}$  in the solid state; the twist angles about the single bond linking the pyridinium rings of “inside” and “alongside” bipyridinium units are 17 and 4°, respectively; the twist angles about the single bond linking the phenylene rings of the two biphenylene spacers are 32 and 26°, respectively

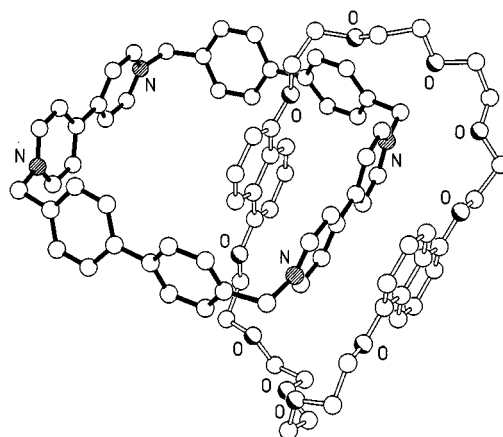


Figure 3. Ball-and-stick representation of the geometry adopted by  $2^{4+}$  in the solid state; the twist angles about the single bond linking the pyridinium rings of “inside” and “alongside” bipyridinium units are 7 and 21°, respectively; the twist angles about the single bond linking the phenylene rings of the two biphenylene spacers are 30 and 28°, respectively

form polar stacks, the “alongside” 1,5-dioxynaphthalene ring system of one molecule being positioned adjacent to the “alongside” bipyridinium unit of the next (the mean interplanar separation is 3.40 Å). Neighboring enantiomerically related stacks are offset with respect to each other in

the polar axis direction though there is a very small overlap of adjacent  $C_i$ -related biphenylene units indicative of some degree of  $[\pi \cdots \pi]$  interaction. The “vacant” region within the tetracationic cyclophane is populated by disordered MeCN solvent molecules.

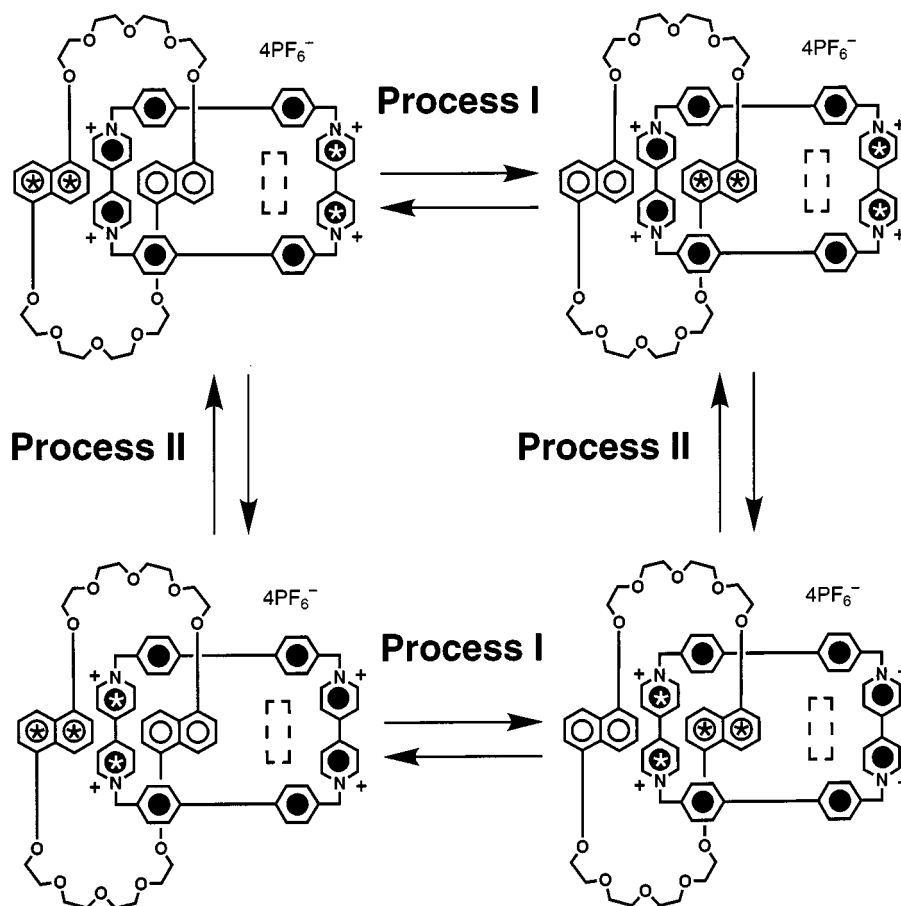


Figure 4. The dynamic processes I and II associated with the [2]catenane  $2 \cdot 4 \text{PF}_6^-$  and with the rotacatenane  $7 \cdot 4 \text{PF}_6^-$ ; the symbol  $\oplus$  is used in order to differentiate the two 1,5-dioxynaphthalene ring systems of the macrocyclic polyether and the two bipyridinium units of the tetracationic cyclophane

<sup>1</sup>H-NMR Spectroscopy

In **2**·4 PF<sub>6</sub>, the circumrotation (process I in Figure 4) of the macrocyclic polyether through the cavity of the tetracationic cyclophane is fast on the <sup>1</sup>H-NMR timescale at 343 K in CD<sub>3</sub>CN. As a result, only three sets of signals for the 1,5-dioxynaphthalene protons H-2/6, H-3/7, and H-4/8 are observed (Figure 5a) in the <sup>1</sup>H-NMR spectrum. On cooling down, process I becomes slow and the three sets of signals separate (Figure 5b) into six sets as “inside” and “alongside” 1,5-dioxynaphthalene ring systems can now be distinguished. By employing the approximate coalescence treatment,<sup>[5]</sup> a free energy barrier of ca. 13 kcal mol<sup>-1</sup> was determined (Table 1) for process I. At 343 K in CD<sub>3</sub>CN, the circumrotation (process II in Figure 4) of the tetracationic cyclophane through the cavity of the macrocyclic polyether is also fast. As a result, the “inside” and “alongside” bipyridinium units cannot be distinguished and only one set of signals is observed (Figure 5a) for the α-bipyridinium protons. On cooling down, process II becomes slow and the set of signals for the α-bipyridinium protons separates into two sets. However, an accurate measurement of the coalescence temperature was not possible and so the free energy barrier associated with process II could not be determined. The local C<sub>2</sub> symmetry associated with the “inside” 1,5-dioxy-

Table 1. Kinetic parameters<sup>[a]</sup> for the dynamic processes associated with the [2]catenane **2**·4 PF<sub>6</sub> and the rotacatenane **7**·4 PF<sub>6</sub> in solution

Compound	Probe protons	Δν <sup>[b]</sup> [Hz]	k <sub>c</sub> <sup>[c]</sup> [s <sup>-1</sup> ]	T <sub>c</sub> <sup>[d]</sup> [K]	ΔG <sub>c</sub> <sup>‡</sup> <sup>[e]</sup> [kcal mol <sup>-1</sup> ]	Process
<b>2</b> ·4 PF <sub>6</sub>	H-2/6	94	209	280	13.4	I
	H-3/7	418	929	291	13.1	I
	H-4/8	1192	2649	309	13.3	I
	α-bipyridinium	146	324	281	13.2	III/ IV
	β-bipyridinium	75	166	276	13.3	III/ IV
<b>7</b> ·4 PF <sub>6</sub>	α-bipyridinium	59	132	183	8.8	V
	H-2/6	322	718	283	12.8	I
	α-bipyridinium	86	191	273	13.1	III/ IV
	α-bipyridinium	93	207	223	10.6	III/ IV

[a] Determined by variable-temperature <sup>1</sup>H-NMR spectroscopy (400 MHz) in (CD<sub>3</sub>)<sub>2</sub>CO. – [b] Limiting frequency separation (error ± 1 Hz). – [c] Rate constant at the coalescence temperature (error ± 5 s<sup>-1</sup>). – [d] Coalescence temperature (error ± 1 K). – [e] Free energy barrier at the coalescence temperature (error ± 0.2 kcal mol<sup>-1</sup>).

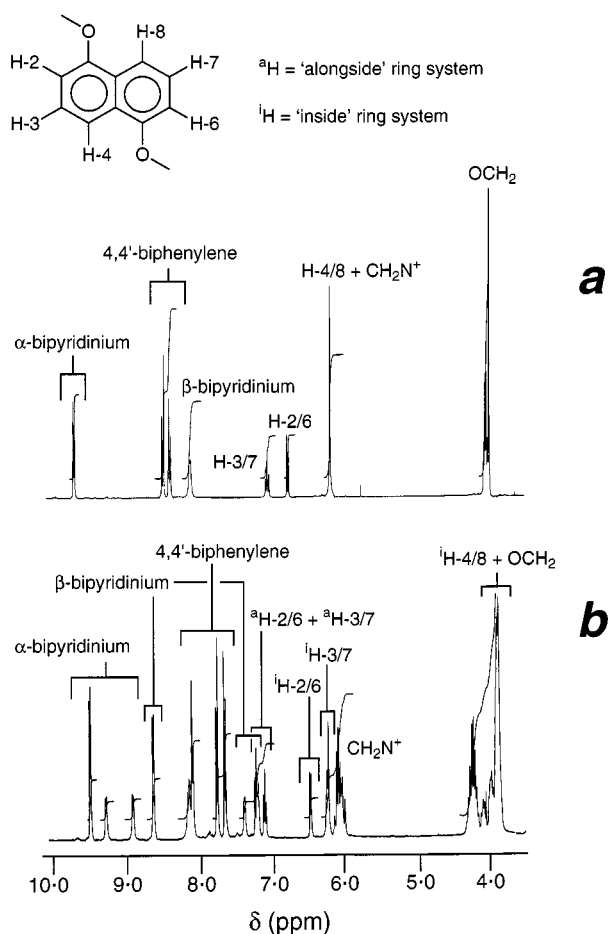


Figure 5. Partial <sup>1</sup>H-NMR spectra of the [2]catenane **2**·4 PF<sub>6</sub> (*a*) in CD<sub>3</sub>CN at 343 K and (*b*) in (CD<sub>3</sub>)<sub>2</sub>CO at 253 K

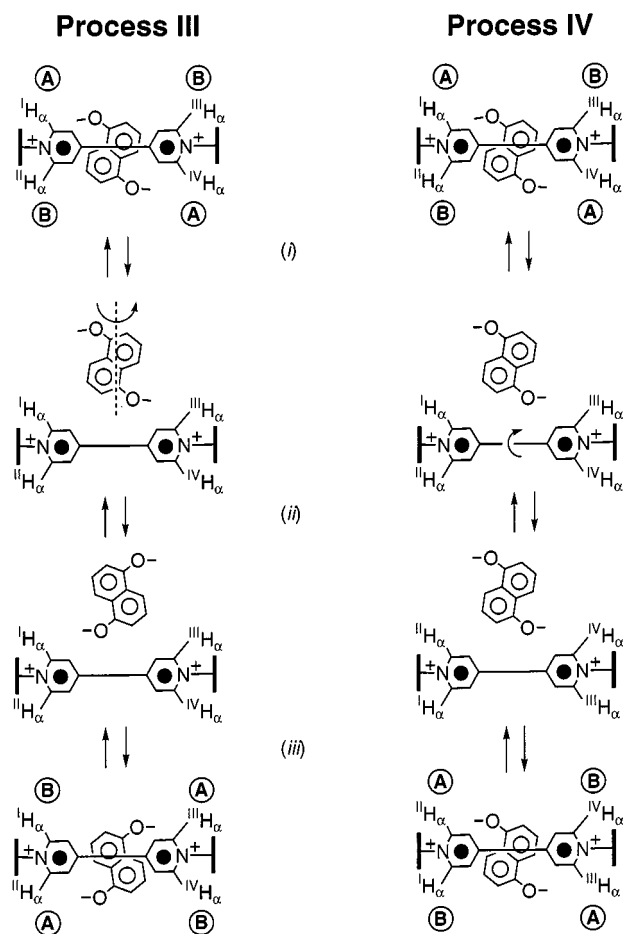


Figure 6. The dynamic processes III and IV associated with the [2]catenane **2**·4 PF<sub>6</sub> and with the rotacatenane **7**·4 PF<sub>6</sub>

naphthalene ring system imposes (Figure 6) two sites (**A** and **B**) on the “inside”  $\alpha$ -bipyridinium protons  $^I\text{H}_a$ – $^{IV}\text{H}_a$ . The protons  $^I\text{H}_a$  and  $^{II}\text{H}_a$ , as well as  $^{III}\text{H}_a$  and  $^{IV}\text{H}_a$ , are exchanged between **A** and **B** as a result of process III and/or process IV. Process III involves (i) dislodgement of the “inside” 1,5-dioxynaphthalene ring system from the cavity of the tetracationic cyclophane, (ii) its 180° rotation about its [O...O] axis, and (iii) its reinsertion inside the cavity of the tetracationic cyclophane. Process IV involves (i) dislodgement of the “inside” 1,5-dioxynaphthalene ring system from the cavity of the tetracationic cyclophane, (ii) 180° rotation of the “inside” bipyridinium unit about its [N...N] axis, and (iii) reinsertion of the 1,5-dioxynaphthalene ring system inside the cavity of the tetracationic cyclophane. At 253 K in  $(\text{CD}_3)_2\text{CO}$ , process III and/or process IV are slow on the  $^1\text{H}$ -NMR timescale and the set of signals associated with the “inside”  $\alpha$ -bipyridinium protons separates (Figures 5b and Figure 7) into two more sets. By employing the approximate coalescence treatment, a free energy barrier of ca. 13 kcal mol $^{-1}$  was determined (Table 1) for process III and/or IV. The local  $C_2$  symmetry associated with the “inside” 1,5-dioxynaphthalene ring system imposes (Figure 8) two sites (**C** and **D**) on the “alongside”  $\alpha$ -bipyridinium protons  $^V\text{H}_a$ – $^{VIII}\text{H}_a$  as well. Exchange of the protons  $^V\text{H}_a$  and  $^{VI}\text{H}_a$ , as well as  $^{VII}\text{H}_a$  and  $^{VIII}\text{H}_a$ , between **C** and **D** occurs as a result of the 180° rotation (Process V) of the “alongside” bipyridinium unit about its [N...N] axis. Thus, the set of signals observed for the “alongside”  $\alpha$ -bipyridinium protons separates (Figure 7) into two sets on further cooling.

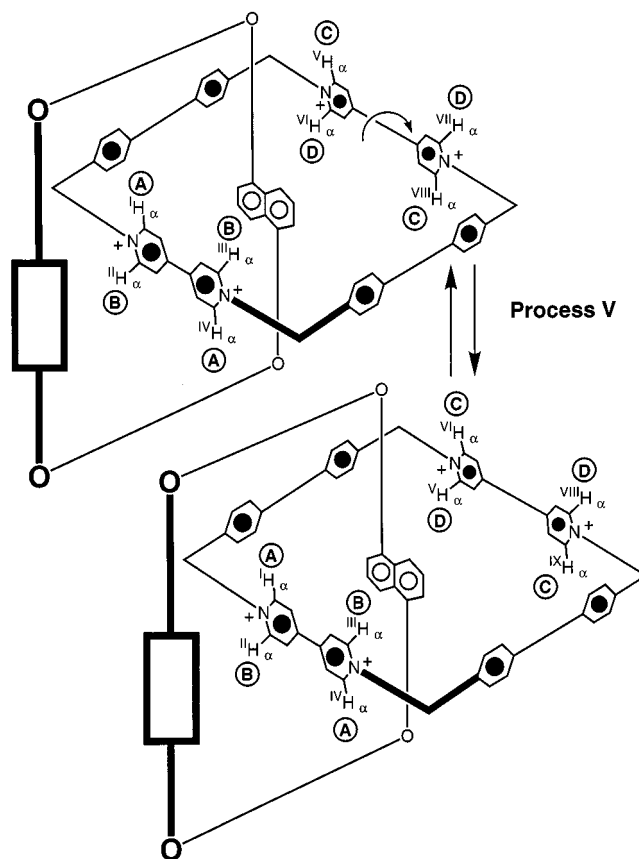


Figure 8. The dynamic process V associated with the [2]catenane **2**·4 PF $_6$

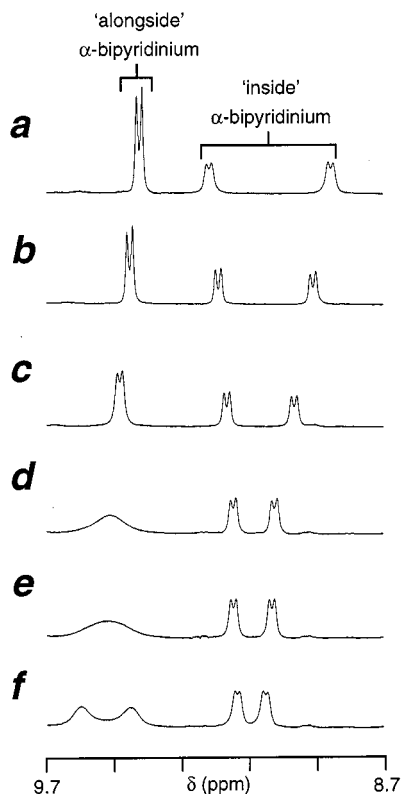


Figure 7. Partial  $^1\text{H}$ -NMR spectra of the [2]catenane **2**·4 PF $_6$  in  $(\text{CD}_3)_2\text{CO}$  at (a) 253, (b) 233, (c) 213, (d) 193, (e) 190, and (f) 183 K

By employing the approximate coalescence treatment, a free energy barrier of 8.8 kcal mol $^{-1}$  was determined (Table 1) for process V at a coalescence temperature of 183 K.

Two co-conformations<sup>[6]</sup> differing in the relative orientations of the “inside” 1,5-dioxynaphthalene ring system, are associated (Figure 9) with the rotacatenane **7**·4 PF $_6$ .<sup>[7]</sup> However, we have not been able to establish if only one co-conformation is present in solution or if both are present and we cannot distinguish between them by  $^1\text{H}$ -NMR spectroscopy. At 213 K in  $(\text{CD}_3)_2\text{CO}$ , the circumrotation (process I in Figure 4) of the macrocyclic polyether through the cavity of the tetracationic cyclophane is slow on the  $^1\text{H}$ -NMR timescale and the protons of the three 1,5-dioxynaphthalene ring systems give rise to nine sets of resonances. On warming the solution up, the six sets of resonances corresponding to the protons of the 1,5-dioxynaphthalene ring systems incorporated into the macrocyclic polyether coalesce into three sets as process I becomes fast. By employing the coalescence treatment, a free energy barrier of 12.8 kcal mol $^{-1}$  was determined (Table 1) for process I at a coalescence temperature of 283 K. The circumrotation (process II in Figure 4) of the tetracationic cyclophane through the cavity of the macrocyclic polyether is also slow on the  $^1\text{H}$ -NMR timescale at 273 K. As a result, two sets of signals are observed for the  $\alpha$ -bipyridinium protons. On cooling the sample solution down, the set of signals corresponding to the bipyridinium unit encircled by the macrocyclic poly-

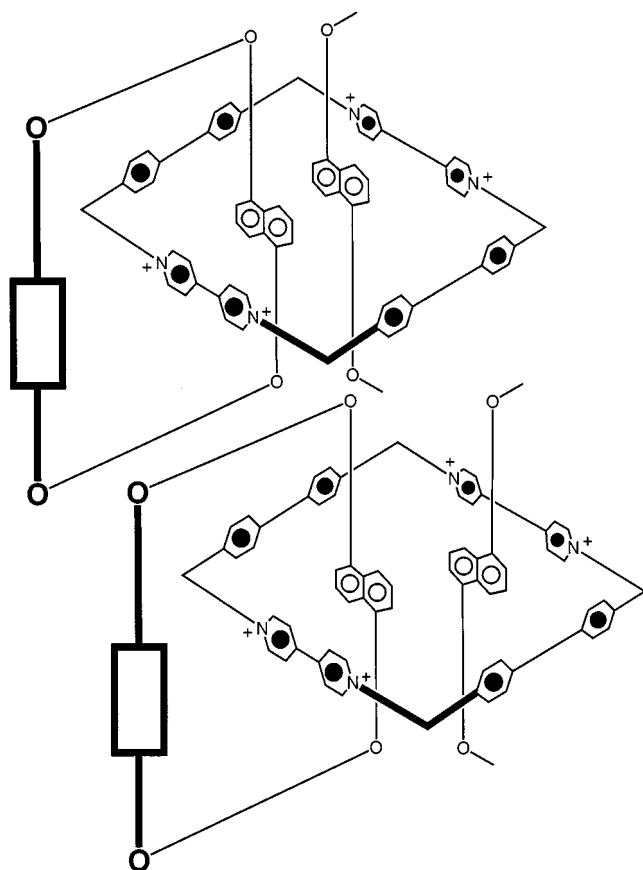


Figure 9. The two co-conformations associated with the different relative orientations of the "inside" 1,5-dioxynaphthalene units of the rotacatenane  $7 \cdot 4 \text{ PF}_6$

ether separates (Figure 10) into two sets as a consequence of the local  $C_2$  symmetry associated with the "inside" 1,5-dioxynaphthalene ring system. Similarly, the set of signals associated with the other bipyridinium unit separates (Figure 10) into two sets at a much lower temperature, again as a result of the local  $C_2$  symmetry associated with the adjacent 1,5-dioxynaphthalene ring system. As for  $2 \cdot 4 \text{ PF}_6$ , the local  $C_2$  symmetry imposed on the  $\alpha$ -bipyridinium protons by the 1,5-dioxynaphthalene ring systems is averaged as a result of co-conformational changes similar to process III and process IV. However, a  $180^\circ$  rotation (cf., process III in Figure 6) of either of the "inside" 1,5-dioxynaphthalene units about their  $[\text{O} \cdots \text{O}]$  axes interconverts the two co-conformations shown in Figure 9 and, thus, is a non-degenerate process. By contrast, averaging of the local  $C_2$  symmetry, without interconversion of the two co-conformations shown in Figure 9, occurs as a result of a  $180^\circ$  rotation (cf. process IV in Figure 6) of either of the bipyridinium units about their  $[\text{N} \cdots \text{N}]$  axes. By employing the coalescence treatment, free energy barriers of 13.1 and 10.6 kcal mol $^{-1}$  were determined (Table 1) at coalescence temperatures of 273 and 223 K, respectively. However, we cannot establish if these energy barriers are associated with degenerate or non-degenerate processes or with a combination of both.

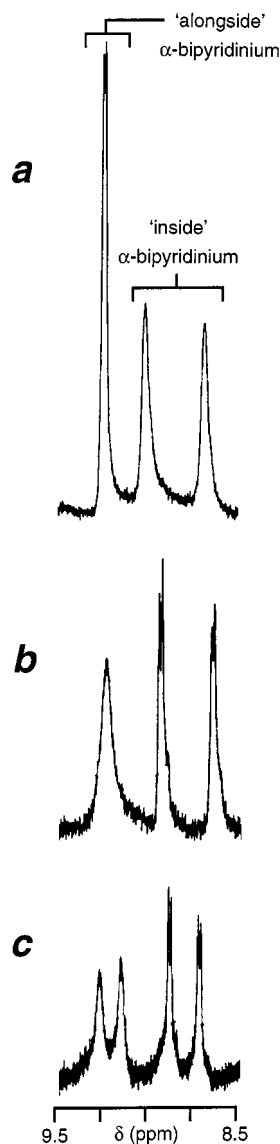


Figure 10. Partial  $^1\text{H}$ -NMR spectra of the rotacatenane  $7 \cdot 4 \text{ PF}_6$  in  $(\text{CD}_3)_2\text{CO}$  at (a) 253, (b) 233, and (c) 213 K

## Conclusions

A [2]catenane incorporating 1,5-dioxynaphtho-38-crown-10 mechanically interlocked with cyclobis(paraquat-4,4'-bi-phenylene) has been synthesized. The cavity of the tetracationic cyclophane component of this [2]catenane is large enough to accommodate one of the 1,5-dioxynaphthalene ring systems of the macrocyclic polyether and also the 1,5-dioxynaphthalene ring systems of an acyclic polyether. Covalent attachment of two bulky groups at both ends of the complexed acyclic polyether converts this supramolecular complex into a mechanically interlocked molecule – a so-called rotacatenane. The structure of the [2]catenane incorporated within this rotacatenane was characterized unequivocally by single-crystal X-ray analysis. Furthermore, variable-temperature  $^1\text{H}$ -NMR-spectroscopic studies carried out on these two compounds led to the determination of the free energy barriers associated with a number of co-

conformational changes occurring in solution. These dynamic processes involve the circumrotation of one macrocyclic component through the cavity of the other and vice versa, the 180° rotations of some of the 1,5-dioxynaphthalene ring systems about their [O...O] axes, and the 180° rotations of the bipyridinium units about their [N...N] axes.

## Experimental Section

**General Methods:** Chemicals were purchased from Aldrich and used as received. Solvents were dried according to literature procedures.<sup>[8]</sup> The compounds 1/5DN38C10,<sup>[9]</sup> **1**·4 PF<sub>6</sub>,<sup>[1]</sup> **3**·2 PF<sub>6</sub>,<sup>[10]</sup> **4**,<sup>[10]</sup> and **6**<sup>[11]</sup> were prepared as described previously in the literature. – Thin layer chromatography (TLC) was carried out on aluminum sheets coated with silica gel 60 (Merck 5554). Column chromatography was performed on silica gel 60 (Merck 9385, 230–400 mesh). – Melting points were determined with an Electrothermal 9200 melting point apparatus and are uncorrected. – Liquid secondary ion mass spectrometry (LSIMS), in conjunction with a 3-nitrobenzyl alcohol or 2-nitrophenyloctyl ether matrix, was performed with a VG Zabspec instrument. For high-resolution LSIMS (HRLSIMS), the instrument operated at a resolution of ca. 6000 by employing narrow-range voltage scanning along with polyethylene glycol or CsI as reference compounds. – <sup>1</sup>H-NMR spectra were recorded with a Bruker AMX400 (400 MHz) spectrometer.

**[2]Catenane 2·4 PF<sub>6</sub> and [3]Catenane 5·4 PF<sub>6</sub>. – Method A:** A solution of 1/5DN38C10 (0.25 g, 0.4 mmol), **3**·2 PF<sub>6</sub> (0.92 g, 1.2 mmol), and **4** (0.40 g, 1.2 mmol) in a mixture of DMF (17 mL) and CH<sub>2</sub>Cl<sub>2</sub> (8 mL) was stirred for 15 d at room temperature. The solvent was distilled off under reduced pressure and the residue was purified by column chromatography [SiO<sub>2</sub>: MeOH/2 M NH<sub>4</sub>Cl<sub>aq</sub>/MeNO<sub>2</sub> (7:2:1)]. The resulting two pure fractions were dissolved in H<sub>2</sub>O individually and NH<sub>4</sub>PF<sub>6</sub> was added to both solutions to afford **2**·4 PF<sub>6</sub> (37 mg, 5%) and **5**·4 PF<sub>6</sub> (86 mg, 10%) as purple solids. **2**·4 PF<sub>6</sub>: M. p. > 300 °C. – LSIMS; *m/z*: 1743 [M – PF<sub>6</sub>]<sup>+</sup>, 1598 [M – 2 PF<sub>6</sub>]<sup>+</sup>, 1453 [M – 3 PF<sub>6</sub>]<sup>+</sup>. – HRLSIMS; *m/z*: calcd. for [M – PF<sub>6</sub>]<sup>+</sup> (C<sub>84</sub>H<sub>84</sub>F<sub>18</sub>N<sub>4</sub>O<sub>10</sub>P<sub>3</sub>) 1743.5113, found 1743.5152. – <sup>1</sup>H NMR (CD<sub>3</sub>CN, 70 °C): δ = 8.76 (8 H, d, *J* = 9 Hz), 7.84–7.67 (16 H, m), 7.42 (8 H, br. s), 6.54–6.50 (4 H, m), 6.29 (4 H, d, *J* = 9 Hz), 5.80–5.70 (12 H, m), 3.96–3.90 (32 H, m). **5**·4 PF<sub>6</sub>: M. p. > 300 °C. – LSIMS; *m/z*: 2381 [M – PF<sub>6</sub>]<sup>+</sup>, 2236 [M – 2 PF<sub>6</sub>]<sup>+</sup>, 2091 [M – 3 PF<sub>6</sub>]<sup>+</sup>. – <sup>1</sup>H NMR [(CD<sub>3</sub>)<sub>2</sub>CO/CD<sub>3</sub>CN, –60 °C]: δ = 8.88 (4 H, d), 8.54 (4 H, d), 8.21–7.92 (8 H, m), 7.89 (8 H, d), 7.02 (4 H, d), 6.93 (4 H, t), 6.91 (4 H, d), 6.69 (4 H, d), 6.30 (4 H, d), 6.02 (4 H, d), 5.74 (4 H, d), 5.50 (4 H, d), 5.24 (4 H, t), 3.72 (4 H, d), 4.15–3.49 (64 H, m).

**Method B:** A solution of 1/5DN38C10 (0.20 g, 0.3 mmol), **3**·4 PF<sub>6</sub> (0.73 g, 0.9 mmol), and **4** (0.32 g, 0.9 mmol) in MeCN (10 mL) was stirred for 18 d at room temperature. The solvent was distilled off under reduced pressure and the residue was purified as described in Method A to afford **2**·4 PF<sub>6</sub> (44 mg, 8%) and **5**·4 PF<sub>6</sub> (280 mg, 35%) as purple solids.

**Method C:** A solution of 1/5DN38C10 (0.18 g, 0.3 mmol), **3**·4 PF<sub>6</sub> (0.65 g, 0.8 mmol), and **4** (0.28 g, 0.8 mmol) in MeCN (10 mL) was stirred for 30 d at room temperature. The solvent was distilled off under reduced pressure and the residue was purified as described in Method A to afford **2**·4 PF<sub>6</sub> (44 mg, 8%) and **5**·4 PF<sub>6</sub> (280 mg, 35%) as purple solids.

**Rotacatenane 7·4 PF<sub>6</sub>:** Tris(isopropyl)silyl triflate (105 mg, 0.33 mmol) and 2,6-dimethylpyridine (36 mg, 0.33 mmol) were added

to a stirred solution of **2**·4 PF<sub>6</sub> (29 mg, 0.01 mmol) and **6** (19 mg, 0.03 mmol) in MeCN (2 mL) maintained at 0 °C and under N<sub>2</sub>. After 2 h, the solvent was distilled off under reduced pressure and the residue was washed with H<sub>2</sub>O and Et<sub>2</sub>O before being dissolved in Me<sub>2</sub>CO. After filtration, the solvent was distilled off under reduced pressure and the residue was purified by column chromatography [SiO<sub>2</sub>: MeOH/2 M NH<sub>4</sub>Cl<sub>aq</sub>/MeNO<sub>2</sub> (7:2:1)]. The resulting purple solid was dissolved in H<sub>2</sub>O and NH<sub>4</sub>PF<sub>6</sub> was added to afford **7**·4 PF<sub>6</sub> (16 mg, 40%) as a purple solid. **8**·4 PF<sub>6</sub>: M. p. > 300 °C. – LSIMS; *m/z*: 2481 [M – PF<sub>6</sub>]<sup>+</sup>, 2335 [M – 2 PF<sub>6</sub>]<sup>+</sup>, 2191 [M – 3 PF<sub>6</sub>]<sup>+</sup>. – HRLSIMS; *m/z*: calcd. for [M – 2 PF<sub>6</sub>]<sup>+</sup> (C<sub>123</sub><sup>13</sup>C<sub>1</sub>H<sub>156</sub>F<sub>12</sub>N<sub>4</sub>O<sub>18</sub>P<sub>2</sub>Si<sub>2</sub>) 2336.0080, found 2336.0090. – <sup>1</sup>H NMR [(CD<sub>3</sub>)<sub>2</sub>CO, –60 °C]: δ = 9.34 (2 H, br. s), 9.20 (2 H, br. s), 8.92 (2 H, br. s), 8.71 (2 H, br. s), 8.30–7.90 (16 H, m), 7.10–6.80 (12 H, m), 6.31 (2 H, d, *J* = 7 Hz), 6.10–6.00 (4 H, m), 5.90–5.78 (4 H, m), 5.67 (2 H, br. s), 5.60–5.48 (4 H, m), 5.37–5.25 (2 H, m), 4.40–3.40 (60 H, m), 1.10–0.90 (42 H, s).

**X-ray Crystallography:** Single crystals of **1**·4 PF<sub>6</sub> and **2**·4 PF<sub>6</sub>, suitable for X-ray crystallographic analysis, were grown by vapor diffusion of *i*Pr<sub>2</sub>O into an MeCN solution of the [2]catenane. **1**·4 PF<sub>6</sub>: [C<sub>102</sub>H<sub>106</sub>N<sub>4</sub>O<sub>15</sub>][PF<sub>6</sub>]<sub>4</sub>·2 MeCN, *M* = 2289.9, triclinic, space group *P* $\bar{1}$  (no. 2), *a* = 13.964(3), *b* = 17.915(4), *c* = 28.368(8) Å, α = 86.46(2), β = 77.24(2), γ = 76.20(2)°, *V* = 6722(3) Å<sup>3</sup>, *Z* = 2, *D*<sub>c</sub> = 1.131 g cm<sup>–3</sup>, μ(Cu-*K*<sub>α</sub>) = 12.7 cm<sup>–1</sup>, *F*(000) = 2372, *T* = 293 K; red blocks, 0.53 × 0.53 × 0.43 mm, Siemens P4/PC diffractometer, graphite-monochromated Cu-*K*<sub>α</sub> radiation, λ = 1.54178 Å, ω-scans, 13826 independent reflections. The structure was solved by direct methods and the non-hydrogen atoms of the crown ether and hexafluorophosphate components refined anisotropically using full-matrix least squares based on *F*<sup>2</sup> to give *R*<sub>1</sub> = 0.298, *wR*<sub>2</sub> = 0.653 for 4831 independent observed reflections [*I*<sub>o</sub> > 4 σ(*I*<sub>o</sub>)], 2θ = 100° and 1006 parameters. As indicated in the text the crystals, and thus the resulting data, were of very poor quality and this, coupled with high thermal vibration/disorder of the hexafluorophosphate anions, solvent and portions of the crown ether lying “outside” the tetracationic cyclophane, resulted in the high final value of *R*<sub>1</sub>. Though the “disordered” regions of the structure have been subjected to geometric optimization, the gross structure is correct. **2**·4 PF<sub>6</sub>: [C<sub>84</sub>H<sub>84</sub>N<sub>4</sub>O<sub>10</sub>][PF<sub>6</sub>]<sub>4</sub>·10.5 MeCN, *M* = 2320.5, triclinic, space group *P* $\bar{1}$  (no. 2), *a* = 16.160(3), *b* = 16.716(3), *c* = 24.770(4) Å, α = 93.41(1), β = 108.54(1), γ = 114.02(1)°, *V* = 5655(2) Å<sup>3</sup>, *Z* = 2, *D*<sub>c</sub> = 1.363 g cm<sup>–3</sup>, μ(Cu-*K*<sub>α</sub>) = 15.0 cm<sup>–1</sup>, *F*(000) = 2406, *T* = 173 K; ruby prisms, 0.73 × 0.73 × 0.17 mm, Siemens P4/RA diffractometer, graphite-monochromated Cu-*K*<sub>α</sub> radiation, λ = 1.54178 Å, ω-scans, 15203 independent reflections. The structure was solved by direct methods and the non-hydrogen atoms refined anisotropically using full-matrix least squares based on *F*<sup>2</sup> to give *R*<sub>1</sub> = 0.105, *wR*<sub>2</sub> = 0.268 for 9053 independent observed reflections [*I*<sub>o</sub> > 4 σ(*I*<sub>o</sub>)], 2θ = 115° and 1451 parameters. – Crystallographic data (excluding structure factors) for the structures reported in this paper have been deposited with the Cambridge Crystallographic Data Centre as supplementary publication no. CCDC-112054 (**1**·4 PF<sub>6</sub>) and -112055 (**2**·4 PF<sub>6</sub>). Copies of the data can be obtained free of charge on application to CCDC, 12 Union Road, Cambridge CB2 1EZ, UK [Fax: int. code + 44(1223)336-033; E-mail: deposit@ccdc.cam.ac.uk].

## Acknowledgments

We thank the Engineering and Physical Sciences Research Council in the United Kingdom for financial support.

- [1] D. B. Amabilino, P. R. Ashton, V. Balzani, S. E. Boyd, A. Credi, J. Y. Lee, S. Menzer, J. F. Stoddart, M. Venturi, D. J. Williams, *J. Am. Chem. Soc.* **1998**, *120*, 4295–4307.
- [2] For accounts, books, and reviews on mechanically interlocked molecules, see: [2a] G. Schill, *Catenanes, Rotaxanes and Knots*, Academic Press, New York, **1971**. — [2b] D. M. Walba, *Tetrahedron* **1985**, *41*, 3161–3212. — [2c] C. O. Dietrich-Buchecker, J.-P. Sauvage, *Chem. Rev.* **1987**, *87*, 795–810. — [2d] J.-P. Sauvage, *Acc. Chem. Res.* **1990**, *23*, 319–327. — [2e] C. O. Dietrich-Buchecker, J.-P. Sauvage, *Bioorg. Chem. Front.* **1991**, *2*, 195–248. — [2f] J.-C. Chambron, C. O. Dietrich-Buchecker, J.-P. Sauvage, *Top. Curr. Chem.* **1993**, *165*, 131–162. — [2g] F. Bickelhaupt, *J. Organomet. Chem.* **1994**, *475*, 1–14. — [2h] D. B. Amabilino, J. F. Stoddart, *Chem. Rev.* **1995**, *95*, 2725–2828. — [2i] F. Vögtle, T. Dünwald, T. Schmidt, *Acc. Chem. Res.* **1996**, *29*, 451–460. — [2j] A. C. Benniston, *Chem. Soc. Rev.* **1996**, *25*, 427–435. — [2k] M. Fujita, K. Ogura, *Coord. Chem. Rev.* **1996**, *148*, 249–264. — [2l] R. Jäger R., F. Vögtle, *Angew. Chem. Int. Ed. Engl.* **1997**, *36*, 930–944. — [2m] M. Belohradsky, F. M. Raymo, J. F. Stoddart, *Collect. Czech. Chem. Commun.* **1997**, *62*, 527–557. — [2n] S. A. Nepogodiev, J. F. Stoddart, *Chem. Rev.* **1998**, *98*, 1959–1976. — [2o] D. G. Hamilton, J. E. Davies, L. Prodi, J. K. M. Sanders, *Chem. Eur. J.* **1998**, *4*, 608–620. — [2p] J.-C. Chambron, J.-P. Sauvage, *Chem. Eur. J.* **1998**, *4*, 1362–1366.
- [3] For accounts and reviews on the template-directed syntheses of catenanes and rotaxanes incorporating  $\pi$ -electron-rich and -deficient components, see: [3a] D. Philp, J. F. Stoddart, *Synlett* **1991**, 445–458. — [3b] D. Pasini, F. M. Raymo, J. F. Stoddart, *Gazz. Chim. Ital.* **1995**, *125*, 431–443. — [3c] D. B. Amabilino, F. M. Raymo, J. F. Stoddart, *Comprehensive Supramolecular Chemistry*, vol. 9 (Eds.: M. W. Hosseini, J.-P. Sauvage), Pergamon, Oxford, **1996**, p. 85–130. — [3d] F. M. Raymo, J. F. Stoddart, *Pure Appl. Chem.* **1996**, *68*, 313–322. — [3e] R. E. Gillard, F. M. Raymo, J. F. Stoddart, *Chem. Eur. J.* **1997**, *3*, 1933–1940. — [3f] F. M. Raymo, J. F. Stoddart, *Pure Appl. Chem.* **1997**, *69*, 1987–1997. — [3g] F. M. Raymo, J. F. Stoddart, *Chemtracts* **1998**, *11*, 491–511.
- [4] For the template-directed syntheses of the [3]catenane **5** · 4 PF<sub>6</sub>, see: P. R. Ashton, C. L. Brown, E. J. T. Chrystal, T. T. Goodnow, A. E. Kaifer, K. P. Parry, A. M. Z. Slawin, N. Spencer, J. F. Stoddart, D. J. Williams, *Angew. Chem. Int. Ed. Engl.* **1991**, *30*, 1039–1042.
- [5] I. O. Sutherland, *Annu. Rep. NMR Spectrosc.* **1971**, *4*, 71–235.
- [6] For a definition of the term “co-conformation”, see: M. C. T. Fyfe, P. T. Glink, S. Menzer, J. F. Stoddart, A. J. P. White, D. J. Williams, *Angew. Chem. Int. Ed. Engl.* **1997**, *36*, 2068–2070.
- [7] For a similar type of isomersim in [3]catenanes, see: P. R. Ashton, S. E. Boyd, C. G. Claessens, R. E. Gillard, S. Menzer, J. F. Stoddart, M. S. Tolley, A. J. P. White, D. J. Williams, *Chem. Eur. J.* **1997**, *3*, 788–798.
- [8] B. S. Furniss, A. J. Hannaford, P. W. G. Smith, A. R. Tatchell, *Practical Organic Chemistry*, Longman, New York, **1989**.
- [9] P. R. Ashton, E. J. T. Chrystal, J. P. Mathias, K. P. Parry, A. M. Z. Slawin, N. Spencer, J. F. Stoddart, D. J. Williams, *Tetrahedron Lett.* **1987**, *28*, 6367–6370.
- [10] D. B. Amabilino, P. R. Ashton, C. L. Brown, E. Córdova, L. A. Godínez, T. T. Goodnow, A. E. Kaifer, S. P. Newton, M. Pietraszkiewicz, D. Philp, F. M. Raymo, A. S. Reder, M. T. Rutland, A. M. Z. Slawin, N. Spencer, J. F. Stoddart, D. J. Williams, *J. Am. Chem. Soc.* **1995**, *117*, 1271–1293.
- [11] P. R. Ashton, J. Huff, S. Menzer, I. W. Parsons, J. A. Preece, J. F. Stoddart, M. S. Tolley, A. J. P. White, D. J. Williams, *Chem. Eur. J.* **1996**, *2*, 31–44.

Received December 17, 1998  
[O98566]